Study of Diffraction at 30 GHz, 140 GHz, and 300 GHz

Chia-Lin Cheng, Seunghwan Kim, and Alenka Zajić
Georgia Institute of Technology, Atlanta, GA 30332 USA

***Abstract*— This paper presents comparison between measurements and modeling of diffraction in indoor obstructed propagation environments at 30 GHz, 140 GHz, and 300 GHz. The results show that all three frequency bands experience diffraction in obstructed environment. Furthermore, the good agreement between measurements and modeling shows that diffraction at mm-wave and THz frequencies can be modeled by using Uniform Geometrical Theory of Diffraction (UTD). Finally, the results show that diffraction becomes more dominant as frequencies increase from mm-wave to THz frequencies.**

I. Introduction

Millimeter-wave frequency band (30-300 GHz) provides abundant unlicensed spectrum and promises to deliver multi-gigabit-per-second data rates for the development of the fifth generation (5G) wireless communication systems [1]–[3]. Lower mm-wave frequencies (26.5-40 GHz) have a potential to improve data rates for 5G cellular systems. Frequencies around 60 GHz have a potential to offer back-haul connection in base stations as well as between small cells [4]. In addition to 30 GHz and 60 GHz frequency bands, D-band (110-170 GHz) is ideally suited for short- and medium-range communications in applications such as velocity sensors and passive millimeter-wave cameras [5], [6]. Finally, 300 GHz frequency band offers an unregulated bandwidth of 47 GHz and can enable novel applications such as pico-cell cellular links and on-body communication for health monitoring systems [7], [8].

All these new applications require good understanding of propagation mechanisms across all millimeter-wave frequencies in order to determine suitable carrier frequencies and to create reliable systems. Additional challenges arise when these systems are brought to motion and propagation conditions vary over time. At mm-wave frequencies, it is very likely that line-of-sight (LoS) path will be partially (or fully) obstructed by objects in the channel, as users change their positions. In contrast to lower frequency bands, where these objects would create multiple reflections, at mm-wave frequencies, in addition to multiple reflections, diffraction can be prevalent propagation mechanism. Hence, it is very important to study impact of diffraction on channel propagation and how to properly account for this effect in channel models. This paper presents measurements at 30 GHz, 140 GHz, and 300 GHz in obstructed indoor propagation environments. The results show that all three frequency bands experience diffraction in obstructed environments, but the diffraction effects become more prominent as frequency increases. Furthermore, it was shown that Uniform Geometrical Theory of Diffraction (UTD) can be used across several frequency bands to model diffraction in obstructed line-of-sight (OLoS) environments.

This work has been supported by NSF grant 1651273. The views and findings in this paper are those of the authors and do not necessarily reflect the views of NSF.

The remainder of the paper is organized as follows. Section II describes the measurement setup and propagation scenarios used to perform measurements. Section III compares measured results with UTD modeling results. Finally, Section IV provides some concluding remarks.

II. Measurement Setup and OLoS Measurement Scenarios

This section briefly describes 30 GHz (26.5–40 GHz), 140 GHz (110–170 GHz), and 300 GHz (300–316 GHz) measurement setups used to conduct measurements.

For 30 GHz, the Agilent N5224 PNA vector network analyzer (VNA) is used to provide an input signal from 26.5 to 40 GHz. Two identical horn antennas with 55° half-power beam width (HPBW) and 10 dBi gain are used. The measurement parameters are summarized in the third column of the Table I. For measurements in D-band (110-170 GHz), we have used the same measurement setup as described in [5]. The measurement parameters are summarized in the fourth column of the Table I. For the measurements in the range of 300-320 GHz, we have used the same measurement setup as described in [8] and the measurement parameters are summarized in the fifth column of the Table I.

TABLE I
Measurement Parameters.

Parameters	Symbol	30 GHz	140 GHz	300 GHz
Frequency sweep points	N	801	801	801
Intermediate frequency bandwidth	Δf_{IF}	100 kHz	100 Hz	20 kHz
Average noise floor	P_N	-82 dBm	-85 dBm	-100 dBm
Input signal power	P_{in}	0 dBm	0 dBm	-10 dBm
Start frequency	f_{start}	26.5 GHz	11 GHz	10 MHz
Stop frequency	f_{stop}	40 GHz	17 GHz	20 GHz
Bandwidth	B	13.5 GHz	60 GHz	16 GHz
Center frequency	f_C	33.25 GHz	140 GHz	307 GHz

The OLoS measurement setups for 30 GHz, 140 GHz, and 300 GHz are presented in Figs. 1 (a)–(c), respectively. The cylindrical obstruction that initially blocks the LoS was gradually moved away from the LoS along a trajectory perpendicular to the LoS. A ceramic mug with diameter of 8.5 cm is used as obstruction for 30 GHz band and 140 GHz band. A metal

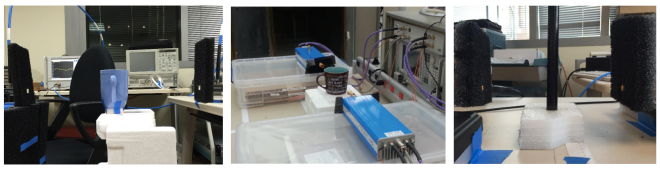

(a) (b) (c)

Fig. 1. OLoS measurement setups at (a) 30 GHz, (b) 140 GHz, and (c) 300 GHz.

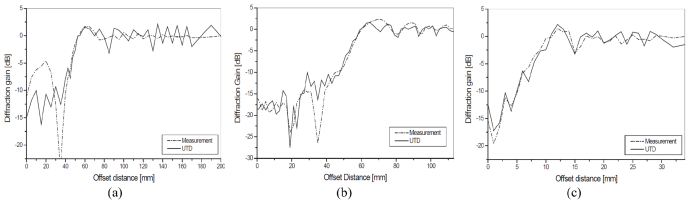

(a) (b) (c)

Fig. 2. Comparison of modeled and measured diffraction gain at (a) 30 GHz, (b) 140 GHz, and (c) 300 GHz.

pipe with diameter of 1.6 cm is used for 300 GHz band in order to accommodate the narrower beam width of 300 GHz antennas. The OLoS measurements at 30 GHz have the Tx–Rx separation distance 40 cm and the obstruction is diagonally moved from 0 to 200 mm off the midpoint with offset step of 5 mm. The OLoS measurements at 140 GHz have the Tx–Rx separation distance 86.36 cm and the obstruction is moved from 0 to 200 mm off the midpoint of LoS with diagonal offset step of 2 mm. The OLoS measurements at 300 GHz have the Tx–Rx separation distance 20 cm and the obstruction is moved from 0 to 34 mm off the midpoint of LoS with diagonal offset step of 1 mm.

III. Comparison of Measured and Modeled Diffraction Gain

To verify existence of diffraction in OLoS at 30 GHz, 140 GHz, and 300 GHz bands, we compare the calculated UTD-diffraction gain using method in [9], [10] to the measured diffraction gain with respect to the cylindrical offset distances. The results in Figs. 2 (a)–(c) show that the predicted UTD models align well with the measured diffraction gain in all frequency bands. Note that in the Shadow Region of 30 GHz channel, i.e., LoS channel is completely blocked by the cylindrical objects, the measured diffraction gain deviates 10 dB from the predicted UTD model. On the other hand, this deviation is not observed in 140 GHz and 300 GHz bands. The reason for deviation is the fact that cylindrical obstruction is more transparent to waves at 30 GHz than at 140 GHz and 300 GHz bands. Another interesting observation is that 10 dB "dip" appears near the shadow-lit boundary in the measured diffraction gain at 30 GHz and 140 GHz. The observed "dip", or abrupt increase in diffraction loss is a result of extra attenuation induced by the thickness of the ceramic mugs wall. As the offset distance increases to 35 mm, where LoS is tangent with the ceramic mug, the fields have to propagate the longest distance through the ceramic material, and therefore, experience the largest attenuation. On the other hand, the "dip" is not observed in the 300 GHz because the increment of the offset step, i.e., 1 mm, is greater than the thickness of the metal pipe, such that the measurement instance does not capture the moment when the "dip" occurs.

In summary, the excellent match between modeled and measured diffraction gain confirms the existence of diffraction at 30 GHz, 140 GHz, and 300 GHz. Compared across frequency bands, 300 GHz band has the best match between measurement results and UTD model. We can conclude that the UTD model works best in scenarios where cylindrical obstructions are least penetrable to the targeted frequency bands, the wall of the cylindrical obstruction should be as thin as possible, and the diameter of the cylindrical obstruction should accommodate the signal beam width.

IV. Conclusions

This paper presents measurements in indoor obstructed propagation environments at 30 GHz, 140 GHz, and 300 GHz. The results show that all three frequency bands experience diffraction in obstructed environment. The good agreement between measurements and modeling shows that diffraction at mm-wave and THz frequencies can be modeled using Uniform Geometrical Theory of Diffraction and that diffraction becomes more dominant effect as frequencies increase from mm-wave to THz.

References

[1] Z. Pi and F. Khan, "An introduction to millimeter-wave mobile broadband systems," *IEEE Communications Magazine*, vol. 49, no. 6, pp. 101–107, June 2011.

[2] T. S. Rappaport, S. Sun, R. Mayzus, H. Zhao, Y. Azar, K. Wang, G. N. Wong, J. K. Schulz, M. Samimi, and F. Gutierrez, "Millimeter wave mobile communications for 5g cellular: It will work!" *IEEE Access*, vol. 1, pp. 335–349, 2013.

[3] Q. C. Li, H. Niu, A. T. Papathanassiou, and G. Wu, "5g network capacity: Key elements and technologies," *IEEE Vehicular Technology Magazine*, vol. 9, no. 1, pp. 71–78, March 2014.

[4] G. R. MacCartney, J. Zhang, S. Nie, and T. S. Rappaport, "Path loss models for 5g millimeter wave propagation channels in urban microcells," in *2013 IEEE Global Communications Conference (GLOBECOM)*, Dec 2013, pp. 3948–3953.

[5] S. Kim, W. T. Khan, A. Zajić, and J. Papapolymerou, "D-band channel measurements and characterization for indoor applications," *IEEE Transactions on Antennas and Propagation*, vol. 63, no. 7, pp. 3198–3207, July 2015.

[6] T. Kosugi, M. Tokumitsu, K. Murata, T. Enoki, H. Takahashi, A. Hirata, and T. Nagatsuma, "120-ghz tx/rx waveguide modules for 10-gbit/s wireless link system," in *2006 IEEE Compound Semiconductor Integrated Circuit Symposium*, Nov 2006, pp. 25–28.

[7] C. Jastrow, K. Munter, R. Piesiewicz, T. Kurner, M. Koch, and T. Kleine-Ostmann, "300 ghz transmission system," *Electronics Letters*, vol. 44, no. 3, pp. 213–214, January 2008.

[8] S. Kim and A. G. Zajić, "Statistical characterization of 300-ghz propagation on a desktop," *IEEE Transactions on Vehicular Technology*, vol. 64, no. 8, pp. 3330–3338, Aug 2015.

[9] S. Kim and A. Zajic, "Utd-based modeling of diffraction loss by dielectric circular cylinders at d-band," in *2016 IEEE International Symposium on Antennas and Propagation (APSURSI)*, June 2016, pp. 1365–1366.

[10] D. McNamara, C. Pistorius, and J. Malherbe, *Introduction to the Uniform Geometrical Theory of Diffraction*, ser. Artech House microwave library. Artech House, 1990. [Online]. Available: https://books.google.com/books?id=bn6pQgAACAAJ